



HAL
open science

Characterization of the grapevine Shaker K⁺ channel VvK3.1 supports its function in massive potassium fluxes necessary for berry potassium loading and pulvinus-actuated leaf movements

Manuel Nieves-Cordones, Mamy-Jean de Dieu Andrianteranagna, Teresa Cuéllar, Isabelle Chérel, Rémy Gibrat, Martin Boeglin, Bertrand Moreau, Nadine Paris, Jean-Luc Verdeil, Sabine Dagmar Zimmermann, et al.

► To cite this version:

Manuel Nieves-Cordones, Mamy-Jean de Dieu Andrianteranagna, Teresa Cuéllar, Isabelle Chérel, Rémy Gibrat, et al.. Characterization of the grapevine Shaker K⁺ channel VvK3.1 supports its function in massive potassium fluxes necessary for berry potassium loading and pulvinus-actuated leaf movements. *New Phytologist*, 2019, 222 (1), pp.286-300. 10.1111/nph.15604 . hal-02054484

HAL Id: hal-02054484

<https://hal.science/hal-02054484>

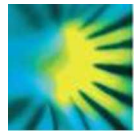
Submitted on 6 Jan 2021

HAL is a multi-disciplinary open access archive for the deposit and dissemination of scientific research documents, whether they are published or not. The documents may come from teaching and research institutions in France or abroad, or from public or private research centers.

L'archive ouverte pluridisciplinaire **HAL**, est destinée au dépôt et à la diffusion de documents scientifiques de niveau recherche, publiés ou non, émanant des établissements d'enseignement et de recherche français ou étrangers, des laboratoires publics ou privés.



Distributed under a Creative Commons Attribution - NonCommercial - NoDerivatives 4.0 International License



**Characterization of the grapevine Shaker K⁺ channel
VvK3.1 supports its function in massive potassium fluxes
necessary for berry potassium loading and pulvinus-
actuated leaf movements**

Journal:	<i>New Phytologist</i>
Manuscript ID	Draft
Manuscript Type:	MS - Regular Manuscript
Date Submitted by the Author:	n/a
Complete List of Authors:	Nieves-Cordones, Manuel; Centro de Edafología y Biología Aplicada del Segura-CSIC, Nutricion Vegetal Andrianteranagna, Mamy; Institut Curie, Institut Curie Cuellar, Teresa; CIRAD, UMR1334 AGAP, PHIV-MRI Gibrat, Remy; BPMP, Univ Montpellier, CNRS, INRA, SupAgro, Montpellier, France, BPMP Boeglin, Martin; BPMP, Univ Montpellier, CNRS, INRA, SupAgro, Montpellier, France, BPMP Moreau, Bertrand; BPMP, Univ Montpellier, CNRS, INRA, SupAgro, Montpellier, France, BPMP Paris, Nadine; BPMP, Univ Montpellier, CNRS, INRA, SupAgro, Montpellier, France, BPMP Verdeil, Jean-Luc; CIRAD, PHIV Zimmermann, Sabine; CNRS Montpellier, Biochimie et Physiologie Moléculaire des Plantes, CNRS, INRA, Montpellier SupAgro, Univ. Montpellier, Gaillard, Isabelle; Univ Montpellier, CNRS, INRA, SupAgro, BPMP
Key Words:	berry K ⁺ loading, paraheliotropic movements, phloem, pulvinus, Shaker K ⁺ channel, VvK3.1 channel

1 **Characterization of the grapevine Shaker K⁺ channel VvK3.1 supports its function in**
2 **massive potassium fluxes necessary for berry potassium loading and pulvinus-**
3 **actuated leaf movements**

4
5
6 M. Nieves-Cordones^{1,3,°}, M. Andrianteranagna^{1,°}, T. Cuéllar², R. Gibrat¹, M. Boeglin¹, B.
7 Moreau¹, N. Paris¹, J.L. Verdeil², S.D. Zimmermann¹ and I. Gaillard^{1*}

8
9
10
11 ¹BPMP, Univ Montpellier, CNRS, INRA, SupAgro, Montpellier, France

12 ²CIRAD, UMR1334 AGAP, PHIV-MRI, 34398, Montpellier Cedex 5, France,

13 ³Present address: Departamento de Nutrición Vegetal, CEBAS-CSIC, Campus de
14 Espinardo, 30100 Murcia, Spain

15
16
17
18
19
20 Running title: Physiological role of the VvK3.1 channel in grapevine

21
22
23 *For correspondence (fax +33 4 67 52 57 37; e-mail isabelle.gaillard@inra.fr).

24 ° MNC and MA have contributed equally to this work

25
26
27
28
29
30 Total word count: 6006

31
32 Word counts for: -Introduction: 859

33 -Materials and Methods: 1119

34 -Results: 1562

35 -Discussion: 2432

36 -Acknowledgements: 34

37 Number of figures: 8

38 Figures 1, 3 and 4 should be published in color

39 Number of Supplemental figures: 5

40 Figures S1, S2 and S5 should be published in color

41 Number of tables: 1

42
43
44
45
46
47
48
49
50
51
52
53
54
55
56
57
58
59
60
61
62
63
64
65
66

Summary (200 words)

- In grapevine, climate changes lead to increased berry potassium (K^+) contents that result in must with low acidity. Consequently, wines are becoming 'flat' to the taste, with poor organoleptic properties and low potential aging, resulting in significant economic loss. Precise investigation of the molecular determinants controlling berry K^+ accumulation during its development are only now emerging.
- Here, we report functional characterization by electrophysiology of a new grapevine Shaker-type K^+ channel, VvK3.1. The analysis of VvK3.1 expression patterns was performed by qPCR and *in situ* hybridization.
- We found that VvK3.1 belongs to the AKT2 channel phylogenetic branch and is a weakly rectifying channel mediating both inward and outward K^+ currents. We showed that *VvK3.1* is highly expressed in the phloem and in a unique structure located at the two ends of the petiole, identified as a pulvinus.
- From the onset of fruit ripening, all data support the role of the VvK3.1 channel in the massive K^+ fluxes from the phloem cell cytosol to the berry apoplasm during berry K^+ loading. Moreover, the high amount of *VvK3.1* transcripts detected in the pulvinus strongly suggests a role for this *Shaker* in the swelling and shrinking of motor cells involved in paraheliotropic leaf movements.

Keywords: berry K^+ loading, paraheliotropic movements, phloem, pulvinus, Shaker K^+ channel, VvK3.1 channel.

67

68

69 **Introduction**

70

71 Wines with a high standard of production are widely known for their characteristic flavors
72 that reflect their environment (*e.g.* climate and soils) and their particular varieties. In the
73 past, the climatic characteristics of different wine growing regions were properly taken into
74 account to best adapt the vines to their environment. However, climate change is now
75 affecting viticulture with high temperatures and soil water deficits that largely constrain
76 grapevine productivity. Berry properties such as color, flavor, and aroma components are
77 altered by these excessive solar radiation and severe drought conditions. Importantly, the
78 impacts of climate change also result in unbalanced wines with excessively low acidity
79 (Jones *et al.*, 2005; Kodur, 2011).

80 Grape acidity results from the ratio between free organic acids (*i.e.* malic and tartaric
81 acids) and organic acids neutralized by potassium (K^+) ions. In grapevine berries, K^+ is
82 involved as a major cellular counter-ion in the electrical neutralization of organic acids, in
83 the control of pH, and in the fine-tuning of the acid-base balance of the flesh cells
84 (Mpelasoka *et al.*, 2003; Kodur, 2011). However, the combined effects of climate change
85 have a reducing effect on the free organic acid content, by increasing the consumption of
86 malic acid as a respiratory substrate (Famiani *et al.*, 2016; Rienth *et al.*, 2016) and favoring
87 K^+ accumulation during the ripening period (Kodur *et al.*, 2011; Duchêne *et al.*, 2014).
88 Excess K^+ then interacts with tartaric acid to form K^+ bitartrate, which precipitates during
89 the winemaking process. This results in musts with low acidity and consequently wines
90 that are too sweet, with strong sensations of wood and alcohol (Mpelasoka *et al.*, 2003).
91 Wine acidity, which normally allows flavor and aroma to develop during winemaking, is
92 essential for the aging potential and also contributes to the red color of wine, through the
93 degree of anthocyanin ionization (Mpelasoka *et al.*, 2003; Davies *et al.*, 2006).

94 The maintenance of berry quality can be achieved by controlling berry K^+ content at
95 harvest. Nevertheless, this requires a better understanding of the molecular basis of K^+
96 accumulation throughout grape berry development, as well as improved identification of
97 the different molecular actors involved in K^+ uptake and accumulation. In plants, K^+
98 accumulation is controlled by multigenic families that encode a broad spectrum of
99 potassium transporters and channels as well as regulatory proteins (protein kinases, protein
100 phosphatases, *etc.*) (Dreyer and Uozumi, 2011; Sharma *et al.*, 2013; Ronzier *et al.*, 2014;
101 Véry *et al.*, 2014; Lefoulon *et al.*, 2016).

102 Among the different K^+ transport systems that have been identified and characterized in
103 grapevine (Pratelli *et al.*, 2002; Davies *et al.*, 2006; Cuéllar *et al.*, 2010, 2013), only two
104 currently appear to be involved in the loading of this cation into grape berries during the
105 ripening stage (Hanana *et al.*, 2007; Cuéllar *et al.*, 2013). The first transport system,
106 VvK1.2 (Cuéllar *et al.*, 2013), is a voltage-gated inwardly rectifying K^+ -selective channel
107 that belongs to the K^+ Shaker channel family. VvK1.2 is specifically expressed in the berry,
108 strongly emerging in the plasma membrane of the flesh cells (mesocarp) and the
109 perivascular cells at veraison (the onset of ripening). Its expression level then continuously
110 increases during berry ripening and can be strongly increased further by mild drought
111 stress. The expression pattern and transcriptional regulation of VvK1.2 both indicate that
112 this channel likely plays a major role in K^+ uptake in flesh cells of ripening berries (Cuéllar
113 *et al.*, 2013). The second transport system, VvNHX1, is a vacuolar cation⁺/H⁺ antiporter
114 belonging to the NHX type of transporter families (Hanana *et al.*, 2007). VvNHX1
115 mediates Na⁺/H⁺ and K⁺/H⁺ coupled exchange, with a higher affinity for K⁺ than Na⁺.
116 Moreover, VvNHX1 expression is strongly increased starting from veraison and during
117 berry maturation, indicating that this transporter may be responsible for vacuolar
118 accumulation of K⁺ at the inception of ripening, driving the uptake of water that generates
119 vacuolar expansion (Hanana *et al.*, 2007).

120 Here, we report the characterization of the grape Shaker K^+ channel VvK3.1. In plants,
121 Shaker genes are known to encode highly K^+ -selective channels that are strongly voltage-
122 regulated. These channels are active at the plasma membrane and provide major pathways
123 for bulk K^+ uptake or secretion in various tissues and cell types (Sharma *et al.*, 2013; Véry
124 *et al.*, 2014). We demonstrate that VvK3.1 is a weak inwardly rectifying K^+ channel that is
125 only slightly activated by CBL-interacting Ser/Thr protein kinase (CIPK)/calcineurin B-
126 like Ca²⁺ sensor (CBL) complexes. This channel is highly expressed in all grapevine
127 organs, with expression restricted to the phloem and phloem parenchyma. We found that
128 VvK3.1 expression in the phloem continuously increases during berry ripening, suggesting
129 a major role for this Shaker channel in the unloading of K^+ from phloem during grape
130 maturation. This is a major concern for grapevines, as the fruit is energetically limited due
131 to stomata disappearance after veraison. Unexpectedly, in addition to the phloem, VvK3.1
132 is expressed in particular structures localized at the joints of the petiole that display the
133 histological features of a pulvinus, *i.e.* a motor organ known to be involved in plant leaf
134 movements. Finally, the roles played by the VvK3.1 channel both in K^+ loading into berry
135 tissues and in grapevine leaf movements are discussed.

136
137

138 **Materials and Methods**

139 **Plant materials**

140 Four-year-old grapevines (*Vitis vinifera* cv. Cabernet Sauvignon) were grown in field
141 conditions within 70-l containers. The controlled watering process used to obtain plants
142 with different water statuses has been described previously (Cuéllar *et al.*, 2010, 2013).
143 Drought conditions were produced by subjecting plants to a reduced irrigation program
144 over a period of 2 weeks, prior to measuring the leaf water potential (ψ) for at least 2 days
145 before tissue collection (Cuéllar *et al.*, 2010). The ψ value ranged from -0.7 to -0.6 MPa in
146 drought-treated plants, whereas ψ remained close to -0.2MPa at dawn for control plants
147 that were not subjected to drought stress. All samples were collected at fruit set period with
148 the exception of berry samples, which were harvested at various stages of grape
149 development. Roots and leaves were collected from 2-month-old rooted canes planted in
150 perlite (Cuéllar *et al.*, 2010). Samples were immediately frozen in liquid nitrogen before
151 being used in the different experiments. For *in situ* hybridization and histology
152 experiments, fresh organs were collected only in the control condition and were directly
153 embedded in paraffin.

154

155 **Isolation of cDNAs encoding VvK3.1, VvCIPK and VvCBL proteins**

156 First strand cDNAs from grapevine were synthesized from total RNA prepared from post-
157 veraison berries using SuperScript III RT polymerase (Invitrogen 18080-051). *VvK3.1* was
158 cloned before the grape genome sequence was made available (Jaillon *et al.*, 2007; Velasco
159 *et al.*, 2007) through a three-step strategy. First, two overlapping EST (expressed sequence
160 tag) sequences (CF518215 and CF519070) corresponding to the 3' region of *VvK3.1*
161 cDNA were identified in the *Vitis vinifera* cv. Cabernet Sauvignon EST library
162 (LIBEST_014375). These were used to design the cf-5' and cf-3' specific primers (Table
163 S1), which amplify a 963 bp fragment. Next, the primers PTK25'-1 and PTK25'-3 were
164 designed based on alignments of group 3 plant Shaker channels identified in different plant
165 species (*Arabidopsis thaliana*, *Solanum lycopersicum*, *Solanum tuberosum*, *Hordeum*
166 *vulgare*;
167 <http://biowed.pasteur.fr/seqanal/interfaces/clustalw.html>). A *VvK3.1* cDNA fragment
168 encoding the conserved domains of the channel's hydrophobic core and its C-terminal
169 domain was amplified through two successive PCR runs with PTK25-1/cf-3' and PTK25'-

170 3/cf3'-2. Finally, 5' RACE was performed to obtain the 5' end of *VvK3.1* cDNA, using the
171 primers AS5, AS6 and AS8.

172 The corresponding full-length clone (GenBank/EMBL XM_002268888.3) was generated
173 by nested PCR using primers flanking the 5' and 3' ends of the coding sequence (first step:
174 full5'kt2f1/full3'KT2R1, second step: full5'KT2atgF2/fullKT2withtaaR2) before
175 subcloning into the PCI vector and verification by sequencing of both strands.

176 *VvCIPK03* (Gene ID: 100241657) and *VvCIPK02/05* (Gene ID: 100261839), the closest
177 relatives of *A. thaliana* CIPK6, were previously cloned (Cuéllar *et al.*, 2013). *VvCBL04*
178 (Gene ID: 100246874), the closest relative of *A. thaliana* CBL4, was cloned through nested
179 PCR using *VvCBL04F1/VvCBL04R1* and *VvCBL04F2/VvCBL04R2* from post-veraison
180 berries. Sequencing of the PCR products confirmed that it corresponds to the expected
181 cDNA.

182

183 **Localization of *VvK3.1* expression by mRNA *in situ* hybridization**

184

185 *In situ* hybridization experiments were performed as described by Cuéllar *et al.* (2010).
186 Briefly, *VvK3.1* RNA probes were synthesized using the *VvK3.1*-specific primers
187 K3.1-124-F/K3.1-124-R (Table S1). An 18S ribosomal probe was used as the control.
188 Sense and antisense probes were labelled with UTP-digoxigenin during the transcription
189 step. Explants from roots, leaves, petioles and berries at different developmental stages
190 were fixed in 4% paraformaldehyde and embedded in paraffin (Cuéllar *et al.*, 2010).
191 Samples were cut into 8- μ m sections and hybridized overnight before incubation for 1 h at
192 37°C in the presence of anti-DIG antibody conjugated with alkaline phosphatase (1/500
193 dilution; Roche, <http://www.roche.com>). Hybridization signals were detected using either
194 the VectorBlue KIT III (Vector Laboratories, <http://www.vectorlabs.com>; positive signal is
195 blue) or the BCIP/NBT substrate system (Dako; positive signal is purple). Slides were
196 observed with a DM600 microscope (Qimaging, <http://www.qimaging.com>) and images
197 were taken with a Qimaging Retiga2000R camera.

198

199 **Histological staining of petiole cross sections**

200 Petioles were fixed for 24 h in a solution containing 1% glutaraldehyde, 2%
201 paraformaldehyde and 1% caffeine in 0.2 mM phosphate buffer at pH 7.2. Subsequently,
202 the samples were dehydrated through an ethanol series, embedded in Technovit 7100 resin

203 (Heraeus Kulzer), and cut into 3- μ m semi-thin sections. These sections were stained with
204 periodic acid-Schiff, which stains polysaccharides (*i.e.* walls and starch) in red, and
205 naphthol blue-black, which stains both soluble and insoluble proteins in blue. Sections
206 were observed by conventional light microscopy using a DM6000 Leica microscope and
207 photographed.

208

209 **Total RNA extraction and real-time quantitative RT-PCR analysis**

210 Total RNA extractions from various tissues (leaves, stems, petioles, tendrils and berries at
211 different developmental stages) were performed using the Plant RNeasy extraction kit
212 (QIAGEN, Germany), using the modifications described in Cuéllar *et al.* (2010). First-
213 strand cDNAs were synthesized with SuperScript III reverse transcriptase (Invitrogen) and
214 used as template for quantitative RT-PCR experiments, as previously described (Cuéllar *et al.*
215 *et al.*, 2010, 2013). Oligonucleotides were designed using Primer3 (<http://frodo.wi.mit.edu/>).
216 Primer pair sequences that are specific to *VvK3.1* (K3.1-124-F/K3.1-124-R) and elongation
217 factor 1-alpha (EF1-F/EF1-R; Cuéllar *et al.*, 2010) are provided in Table S1.

218

219 **Functional characterization of VvK3.1**

220 Oocyte handling and voltage clamp experiments were performed as previously described
221 (Cuéllar *et al.*, 2010, 2013). *VvK3.1* cRNAs (6 ng) were injected using a microinjector
222 (Nanoliter 2000, WPI, <http://www.wpi-europe.com/fr/>) into *Xenopus laevis* oocytes. For
223 co-expression experiments with *VvCIPK03* or 02/05 and *VvCBL04*, the same amount of
224 *CIPK/CBL* (1:1) cRNA was injected. Control oocytes were injected with water (23 nl) or
225 *CIPK/CBL* cRNA. Injected oocytes were maintained at 19°C in a standard solution (ND96;
226 pH 7.4) containing 96 mM NaCl, 2 mM KCl, 1 mM MgCl, 1.8 mM CaCl₂, 5 mM HEPES,
227 and 2.5 mM sodium pyruvate, supplemented with gentamycin sulfate (50 μ g ml⁻¹).
228 Membrane currents were measured 3-5 days after injection with a two-microelectrode
229 voltage clamp amplifier (GeneClamp 500B; Axon Instruments,
230 <http://www.moleculardevices.com>) and a Digidata 1322A interface (Axon Instruments).
231 Pipettes were filled with solutions of 3 M KCl containing 100 (K100), 50 (K50) or 10 mM
232 (K10) potassium gluconate, supplemented respectively with 0, 50 or 90 mM sodium
233 gluconate in 1 mM CaCl₂, 2 mM MgCl₂, and 10 mM HEPES (pH 6.5 or 7.5) or 10 mM
234 MES (pH 5.5). Inhibition by Cs⁺ or Ba²⁺ was assayed by addition of 10 mM CsCl or 30
235 mM BaCl to the K100 solution at pH 6.5. Voltage clamp protocols were applied with 1.4 s
236 voltage pulses from +70 to -155 mV (or -170 mV), in -15 mV steps, followed by a 250-ms

237 voltage step to -40 mV at a holding potential of 0 mV. Normalized current–voltage (I–V)
 238 curves were obtained by plotting steady-state currents at the end of activating voltage
 239 pulses against corresponding applied membrane potentials, setting the current value at -140
 240 mV in K100 at pH 6.5 to -1 for each oocyte. Voltage-pulse protocols, data acquisition and
 241 analysis were performed using the pClamp 10 program suite (Axon Instruments).

242

243

244 **Results**

245

246 **Identification of the grapevine K⁺ channel VvK3.1**

247 Alignments of pore-forming and cyclic nucleotide-binding domains of K⁺ channels cloned
 248 in plants were used to design adequate primers for identifying grapevine homologs of *A.*
 249 *thaliana* Shaker K⁺ channels. A 2,526 bp cDNA was obtained from the total RNA of post-
 250 veraison *Vitis vinifera* (cv. Cabernet Sauvignon) berries, using a combination of reverse
 251 transcription (RT)-PCR amplifications and 5' RACE extension. The deduced amino acid
 252 polypeptide contains 841 residues and shares sequence homology with other plant Shaker
 253 channels. Phylogenetic analysis revealed that this grape *Shaker*, subsequently named
 254 VvK3.1, is related to AKT2 and belongs to group III of the plant Shaker K⁺ family (Fig.
 255 1a). The corresponding polypeptide displays 68% amino acid sequence identity (ASI)
 256 throughout the entire protein length with its *A. thaliana* counterpart, AKT2 (Lacombe *et*
 257 *al.*, 2000). Of particular note is that group III is composed of a single member in both the
 258 *A. thaliana* and grapevine Shaker families. Sequence analysis of the VvK3.1 polypeptide
 259 identified the typical structural regions of Shaker subunits (Fig. 1b), with a short N-
 260 terminal cytosolic domain followed by 6 transmembrane segments. This includes a well-
 261 defined pore region between the fifth and the sixth transmembrane domain which contains
 262 the potassium-selective signature sequence “TXXTXGYGD” (Dreyer *et al.*, 1998). The
 263 large cytosolic C-terminal part begins just after the end of the sixth transmembrane domain
 264 (S6) and successively contains a C-linker domain, a cyclic nucleotide-binding domain
 265 (CNBD), an ankyrin domain, and a K_{HA} domain (Ehrhardt *et al.*, 1997; Sharma *et al.*,
 266 2013; Nieves-Cordones *et al.*, 2014; Véry *et al.*, 2014).

267

268 **The Shaker K⁺ channel gene VvK3.1 is expressed in all tested grapevine organs**

269 To evaluate the expression pattern of the VvK3.1 gene in various grapevine organs, real-
 270 time PCR was performed on total RNA extracted from leaves, stems, petioles, tendrils,

271 roots and berries at different stages of development. High *VvK3.1* transcript levels were
272 detected in all analyzed samples (Fig. 2a). This result is in agreement with the previous
273 observation that group III Shaker subunits (AKT2 branch) display the broadest expression
274 spectrum (Lacombe *et al.*, 2000; Ache *et al.*, 2001; Langer *et al.*, 2002). *VvK3.1* expression
275 in grape berries increased during grape development, reaching a maximal amount in ripe
276 berries (Fig. 2b).

277 To check the *VvK3.1* expression profile at different developmental stages, *in situ*
278 hybridization analyses were conducted in flowers, as well as in berries at the fruit set and
279 ripening (post-veraison) stages (Fig. 3). In flowers, *VvK3.1* transcripts were detected in the
280 phloem (Fig. 3a6). An intense signal was also observed in the inner part of the ovule,
281 named the nucellus, where the embryo sac develops (Fig. 3a4). *VvK3.1* expression was
282 also detected to a lesser extent in the epidermis of ovarian locules and at the base of
283 stigmas (Fig. 3a3-a6). During the fruit set stage in berries, *VvK3.1* expression was mainly
284 detected in the phloem and in the endosperm, a storage tissue that is derived from double
285 fertilization (Fig. 3b2-b4). During the ripening stage (post-veraison period), *VvK3.1*
286 expression was strongly restricted to the phloem and perivascular cells (Fig. 3c3-c5). High
287 levels of *VvK3.1* transcripts were exclusively detected in the phloem of leaves (Fig. S1)
288 and roots (Fig. S2).

289 Interestingly, aside from its expression in the phloem, *VvK3.1* was identified in a structure
290 located at both extremities of the petiole (Fig. 4a1-2, white arrows, and c3-6). When
291 drought stress was applied by stopping plant irrigation, these particular zones of the petiole
292 became curved, bringing the leaf parallel to the stem (Fig. 4a1-2). Histological
293 examination of this part of the petiole (Fig. 4b1-3) revealed an asymmetrical organization
294 with specific cell layers organized around the vascular systems at the abaxial face of the
295 petiole (Fig. 4a4, abs). This organization is consistent with a pulvinus structure, as shown
296 under higher magnification (Fig. 4b). In this zone we observed the presence of two
297 different cell types: small cells with large pectin walls, in the outer cell layers (Fig. 4b2-3,
298 red staining); and thin-walled large parenchyma cells containing a large vacuole, in the
299 innermost cell layers (Fig. 4b-c). It is important to note that *VvK3.1* expression is detected
300 in both of these cell layers (Fig. 4c5). In plants, the pulvini are involved in leaf
301 movements that occur in response to a variety of endogenous and exogenous stimuli
302 (Moran, 2007), although so far this structure has not been described in grapevine.

303

304 **Effect of drought stress on *VvK3.1* expression**

305 The response of grapevine to water stress is highly dependent on the variety and the
 306 rootstock, although a limited water stress is generally considered to be beneficial for berry
 307 quality. It has been demonstrated, from the start of the veraison stage, that grapevine is
 308 relatively tolerant to water deficit. Furthermore, regulated irrigation has been
 309 advantageously used to inhibit vine growth without any reduction in berry yield (Kennedy
 310 *et al.*, 2000; Esteban *et al.*, 2001). Here, the effects of moderate drought stress (-0.7 to -
 311 0.6 MPa for at least 2 days before tissue harvesting) were reproduced in field conditions, as
 312 described above. Berries were sampled after flowering (AF) at three stages of
 313 development: post-fruit set stage (day 25 AF), veraison (day 60 AF), and during ripening
 314 (day 75 AF). *VvK3.1* expression in berries was then investigated by real-time quantitative
 315 PCR (qPCR), and a slight increase in *VvK3.1* transcript levels was observed upon drought
 316 stress (Fig. 5a), particularly in the early stages. Nevertheless, this induction of *VvK3.1*
 317 transcript in response to drought stress was far less considerable than the quantity
 318 previously observed for *VvK1.2* (Cuéllar *et al.*, 2013).

319 *VvK3.1* transcript accumulation was also investigated by qPCR in leaves and roots
 320 harvested from water-stressed or control rooted canes. Drought stress, induced by stopping
 321 irrigation, was found to have different effects on *VvK3.1* transcript levels in roots and
 322 leaves. Specifically, drought stress increased *VvK3.1* transcript accumulation in leaves
 323 (Fig. 5b) but had no effect on the level of *VvK3.1* in roots (Fig. 5c). In leaves, a significant
 324 (threefold) up-regulation in *VvK3.1* was observed in response to water stress.

325

326 ***VvK3.1* behaves as a weak K⁺ inward rectifier channel in *Xenopus* oocytes**

327 Functional properties of the grapevine channel *VvK3.1* were investigated in *Xenopus*
 328 *laevis* oocytes. Instantaneous and time-dependent currents (Fig. 6a) were reminiscent of
 329 those observed with the *A. thaliana* Shaker channel AKT2 previously characterized as a
 330 weak K⁺ inward rectifier channel (Philippart *et al.*, 1999; Lacombe *et al.*, 2000; Ache *et al.*,
 331 2001; Langer *et al.*, 2002). The observed currents were dependent on external potassium
 332 concentrations and exhibited smaller amplitudes at reduced external K⁺ concentrations
 333 (Fig. 6b). Reversal potentials were found to shift towards more hyperpolarized potentials
 334 in response to decreasing K⁺ concentrations (Fig. S3a). *VvK3.1* was inhibited in a voltage-
 335 dependent manner by Cs⁺ (Fig. 6c), with an increase in channel blocking at more negative
 336 potentials as previously described for AKT2 (Lacombe *et al.*, 2000). Addition of 30 mM
 337 Ba²⁺ also provoked a strong inhibition of currents (Fig. S3b), reminiscent of the complete
 338 AKT2 blocking by Ba²⁺ (Marten *et al.*, 1999).

339 Acidification of the external solution reduced VvK3.1 current amplitudes (Fig. 7a), as
340 shown similarly for *A. thaliana* AKT2 channel activity (Lacombe *et al.*, 2000), and in
341 contrast to the behavior of inward rectifiers such as VvK1.2 (Cuéllar *et al.*, 2013). Indeed,
342 VvK3.1 activity was stimulated by an increase in external pH, suggesting an interference
343 of protons with the channel permeation. Upon external acidification, the proportions of
344 instantaneous as well as time-dependent currents were modified. For VvK3.1, inhibition of
345 the time-dependent component was slightly stronger than that of the instantaneous current
346 (Fig. 7b). This should result in a reduced inward rectification capacity of its residual
347 current, whereas the opposite was found for AKT2 (Lacombe *et al.*, 2000).

348 Another level of Shaker K⁺ channel activity regulation is based on CIPK-CBL interactions.
349 Indeed, the *A. thaliana* Shaker channel AKT2 was previously shown to be regulated by the
350 CIPK6/CBL4 complex (calcineurin B-like (CBL)-interacting protein kinase 6 (CIPK) and
351 Ca²⁺-sensing CBL 4 partners) (Held *et al.*, 2011). Since the mechanisms of K⁺ channel
352 regulation involving CIPK-CBL complexes are conserved between *A. thaliana* and
353 grapevine for other Shaker-type channels (Cuéllar *et al.*, 2010, 2013), we also evaluated
354 this regulation for VvK3.1. Thus, cDNAs from VvCIPK03, VvCIPK02/05 and VvCBL04,
355 which are the closest grapevine relatives of *A. thaliana* AtCIPK6 and AtCBL4 (Fig. S4),
356 were cloned from post-veraison berries to assess whether this regulatory pathway is
357 conserved in grapevine. When expressed without the channel, the VvCIPK03/VvCBL04
358 and VvCIPK02/05/VvCBL04 complexes did not elicit any significant currents in oocytes
359 in comparison to water-injected oocytes (Fig. 8a, top). Conversely, even though the
360 VvK3.1 channel was able to mediate K⁺ currents when expressed alone (Fig. 8a, middle),
361 co-expression with these two CIPK/CBL partners led to an increase in the current
362 magnitude (Fig. 8a, bottom). Indeed, co-expression of VvK3.1 together with
363 VvCIPK03/CBL04 significantly increased the K⁺ current by about 60% at -140 mV, in
364 comparison to the current recorded when the VvK3.1 channel was expressed alone in
365 oocytes (Fig. 8b). The other tested CIPK-CBL complex, VvCIPK02/05/VvCBL04,
366 provoked a weaker increase in K⁺ current, by about 20% at -140 mV (Fig. 8b). Finally, it is
367 worth noting that the relative proportions of the instantaneous and time-dependent
368 components of the VvK3.1 currents were not altered by these two CIPK/CBL complexes
369 (Fig. 8C). Similarly, when the AKT2 channel is co-expressed with AtCIPK3-AtCBL4
370 complex, no significant change in the proportion of the two current components is
371 observed (Held *et al.*, 2011).

372

373

374 **Discussion**375 **The grapevine VvK3.1 and *A. thaliana* AKT2 channels share functional properties**

376 In grapevine, VvK3.1 is the only subunit belonging to the third group of Shaker channels
 377 representing a subfamily of weak rectifiers. Similarly, this group contains a single subunit
 378 in *A. thaliana*, named AKT2. With 68% amino acid sequence identity, VvK3.1 is the
 379 closest relative of AKT2 in grapevine (Fig. 1). The *Arabidopsis* AKT2 channel is known to
 380 dominate the phloem K⁺ conductance in both sieve and companion cells, where it has a
 381 major role in phloem K⁺ loading and unloading (Marten *et al.*, 1999; Deeken *et al.*, 2000,
 382 2002; Lacombe *et al.*, 2000; Ache *et al.*, 2001; Philippar *et al.*, 2003; Ivashikina *et al.*,
 383 2005; Hafke *et al.*, 2007). When expressed in *X. laevis* oocytes, the AKT2 channel forms a
 384 weakly rectifying channel, thereby giving rise to two current components with different
 385 gating modes (Marten *et al.*, 1999; Lacombe *et al.*, 2000; Dreyer *et al.*, 2001; Michard *et al.*,
 386 2005a). This unique feature allows AKT2 to mediate inward as well as outward K⁺
 387 currents. As shown in Fig. 8, the VvK3.1 channel can also combine two gating modes: a
 388 time-dependent voltage-activated current, and an instantaneous ohmic current, like AKT2.
 389 Although it has been described that AKT2 can switch between these gating modes *via*
 390 post-translational regulation (Michard *et al.*, 2005a), the underlying mechanisms are still
 391 not fully understood (Sandmann *et al.*, 2011). Two serine residues (S210 and S329), with
 392 one located in the S4–S5 linker and the other in the C-linker, have been identified as
 393 phosphorylation targets (Dreyer *et al.*, 2001; Michard *et al.*, 2005a, 2005b). Moreover, the
 394 lysine (K197) located within the voltage sensor region enables AKT2 to sense its
 395 phosphorylation status and to change between the two modes (Michard *et al.*, 2005b;
 396 Sandmann *et al.*, 2011). Interestingly, these two serines and this lysine are present in the
 397 corresponding position in the VvK3.1 sequence, strongly indicating that VvK3.1 behaves
 398 similar to AKT2.

399 Moreover, in oocytes, the AKT2-like channels are inhibited upon external acidification
 400 (Marten *et al.*, 1999; Philippar *et al.*, 1999; Lacombe *et al.*, 2000; Langer *et al.*, 2002). Our
 401 results demonstrate that the VvK3.1 channel displays a similar pH sensitivity, with one
 402 minor difference: the relative proportions of the instantaneous and time-dependent currents
 403 are differently disturbed as compared to AKT2 (Fig. 7). Indeed, external acidification
 404 results in an increased inward rectification of the AKT2 residual current (Lacombe *et al.*,
 405 2000), whereas under the same conditions the instantaneous component prevails in the

406 VvK3.1 residual currents.

407 In addition, several reports have identified associations between AKT2 and different
408 putative partners (Chérel *et al.*, 2002; Held *et al.*, 2011; Sklodowski *et al.*, 2017). For
409 example, the association of AKT2 with the AtCIPK6/AtCBL4 complex gives rise to an
410 increase in macroscopic AKT2 currents, by enhancing the targeting of AKT2 to the plasma
411 membrane (Held *et al.*, 2011). Since VvK3.1 appears to be closely related to AKT2, we
412 assumed that a homologous regulatory network could control its activity at the cell
413 membrane. In *X. laevis* oocytes, co-expression of VvCBL04 with VvCIPK03 or
414 VvCIPK02/05, the closest relatives respectively of AtCBL4 and AtCIPK6 (Fig. S4)
415 (Cuéllar *et al.*, 2013), produced an increase in the VvK3.1 current. This increase displayed
416 a higher magnitude in the VvCIPK03-VvCBL04 pair (Fig. 8). Moreover, no significant
417 effect on the relative proportions of the instantaneous and time-dependent currents was
418 observed (Fig. 8c), similar to previous observations with AKT2 (Held *et al.*, 2011).
419 Overall, the functional properties of VvK3.1 and AKT2 indicate that these two channels
420 have very similar behaviors, providing additional support to the phylogenetic relationship
421 between them and the group III plant Shaker K⁺ channels. More generally, our results,
422 together with those described earlier for VvK1.1 and VvK1.2 (Cuéllar *et al.*, 2010, 2013),
423 reinforce the observation that the mechanisms of K⁺ channel regulation by CIPK–CBL
424 complexes are conserved between *A. thaliana* and grapevine.

425 **Role of the VvK3.1 channel in berry K⁺ loading**

426 Berry development consists of two successive growth periods. The first period comprises a
427 rapid cell division phase followed by marked cell enlargement. This period is characterized
428 by the synthesis and vacuolar storage of tartaric and malic acids. The second period
429 commences with veraison, at the onset of ripening. At veraison, the berry starts to change
430 color and soften, as it becomes a strong sink for water, K⁺, sugar and solute imports
431 (Davies *et al.*, 2006; Conde *et al.*, 2007). At this stage, berry loading is dependent on
432 phloem sap flux, since the xylem has become non-functional (Keller *et al.*, 2006; Chatelet
433 *et al.*, 2008a, 2008b; Choat *et al.*, 2009; Knipfer *et al.*, 2015). Moreover, K⁺ transport in
434 the berry switches from the symplasmic to the apoplasmic mode (Zhang *et al.*, 2006),
435 meaning that unloaded solutes must cross plasma membranes at least twice before
436 accumulating within the berry mesocarp. Previous research has posited that berry loading
437 *via* an apoplasmic mode should reduce the transport of apoplasmic solutes out of the

438 berries (Findlay *et al.*, 1987; Mpelasoka *et al.*, 2003) and improve the control of efficient
439 long-distance phloem transport from source leaves to ripening berries (Zhang *et al.*, 2006).
440 Starting at veraison, the VvK3.1 channel is highly expressed in the berry phloem (Figs. 2
441 and 3) and becomes the obvious candidate for loading K^+ into the berry. The unique
442 functional characteristics of the VvK3.1 channel are indeed suited for this. In this scenario,
443 the VvK3.1 channel would be switched from an inward-rectifying to a non-rectifying mode,
444 so as to enable massive K^+ efflux, *i.e.* K^+ secretion into the berry mesocarp apoplasm.
445 Taking into account previous studies on AKT2 functioning (Marten *et al.*, 1999; Lacombe
446 *et al.*, 2000; Dreyer *et al.*, 2001; Michard *et al.*, 2005a, 2005b) and the fact that the AKT2
447 and VvK3.1 channels have very similar functional behaviors, VvK3.1 should be locked in
448 the open state in its phosphorylated form across the entire physiological voltage range.
449 Therefore, this channel may drive the K^+ efflux that allows K^+ ions to move down their
450 transmembrane concentration gradient (100 mM in the phloem cell cytoplasm and 1 mM in
451 the apoplasm; Ache *et al.*, 2001; Wada *et al.*, 2008).

452 It is known that K^+ gradients play a major role in driving sugar, amino acid and water
453 transport across plant cell membranes during phloem unloading (Ache *et al.*, 2001;
454 Philippar *et al.*, 2003). However, the remarkable increase in solute import in berries at
455 veraison signifies a challenge in terms of transport energization. Electrochemical gradients
456 dependent on the H^+ -ATPase activity may be reduced in berries since, from the start of
457 veraison, the stomata are no longer functional, photosynthesis has stopped, and ATP
458 synthesis mostly depends on cellular respiration with malic acid as the substrate (Kanellis
459 and Roubelakis-Angelakis, 1993). Under such circumstances, the recent concept of a K^+
460 battery for transmembrane transport processes seems appropriate, since it provides
461 additional energy stored in the K^+ gradient between the phloem cytosol and the berry
462 apoplasm (Gajdanowicz *et al.*, 2011; Sandmann *et al.*, 2011; Dreyer *et al.*, 2017). The K^+
463 battery also explains how an open AKT2-like channel, like VvK3.1, can drive K^+ ions
464 from the cytosol to the apoplasm as well as reinforce the transmembrane electrical gradient
465 by hyperpolarizing the plasma membrane potential. This electrical gradient can
466 compensate for the reduced pH gradient present under energy limitation. Furthermore, it
467 can be used to retrieve sucrose from the apoplasm and to maintain sucrose levels in the
468 phloem vessels until reaching the different sites of unloading.

469 In grapevine, sucrose is used for long-distance transport in the phloem from source leaves
470 to grape berries, and sugar loading into berries is performed from veraison onward and

471 during the ripening period (Kuhn and Grof, 2010; Lecourieux *et al.*, 2014). Anatomical
472 sections of grape berries reveal a large network of vascular bundles with a central capillary
473 bundle and many major and minor peripheral capillary bundles that irrigate the berry
474 (Zhang *et al.*, 2006). This observation strongly suggests that sucrose retrieval could be
475 performed over the entire length of the grape berry's vascular bundle (from the different
476 sites of phloem unloading), in order to distribute the large amount of sucrose to all parts of
477 the berry mesocarp apoplasm.

478 The main advantage of this K^+ battery mechanism is that it does not require ATP
479 consumption (Dreyer *et al.*, 2017). Thus, it is tempting to speculate that the non-rectifying
480 mode of VvK3.1 contributes to K^+ secretion into the grape berry apoplasm, in addition to
481 switching on the K^+ battery to allow sucrose retrieval in energy-limited conditions. At this
482 stage, the inwardly rectifying VvK1.2 channel (Cuéllar *et al.*, 2013) that is highly
483 expressed in flesh cells and perivascular cells surrounding the vascular bundles would then
484 contribute to the berry loading mechanisms. In particular, this Shaker channel is strongly
485 activated by interacting with specific VvCIPK/VvCBL pairs. This can allow rapid
486 absorption of K^+ by perivascular cells and then by flesh cells to keep the apoplasmic
487 K^+ concentration at low levels, despite the efflux from the phloem stream. Indeed, since
488 the transmembrane gradient of K^+ can be maintained between phloem cells and the berry
489 apoplast, the phloem stream flux towards the sink may be stimulated and employment of
490 the K^+ battery process for sucrose retrieval may persist over a long period of time. This
491 latter process should also allow saving ATP, which in grape berry is locally produced by
492 cell respiration, for other transport mechanisms driven by ATP-consuming H^+ -ATPase.

493

494 **VvK3.1 and K^+ transport in the grapevine pulvinus**

495 In addition to the phloem, VvK3.1 is also strongly expressed in a second tissue located at
496 the two ends of the petiole (Fig. 4). The careful histological examination of this zone (Fig.
497 4. a1-2) enabled us to identify this as a specialized motor organ known as the pulvinus.
498 Nastic, paraheliotropic and diaheliotropic movements are mediated by this organ, allowing
499 it to play a key role in leaf movements (Pastenes *et al.*, 2004). Because grapevine is a
500 major crop in both warm and drought-prone areas, this plant has the ability to perform
501 solar tracking in order to reduce leaf temperature and transpirational water loss, and protect
502 its photosynthetic activity. In this context, several studies on the impacts of excess light on
503 the photosynthesis rate in grapevine leaves have been conducted (During, 1988; Iandolino
504 *et al.*, 2013; Keller, 2015). High irradiance induces photodamage to photosystem II (PSII)

505 in leaves (Adir *et al.*, 2003; Pastenes *et al.*, 2004; Takahashi *et al.*, 2009) and leads to
506 photoinhibition, which can limit plant photosynthesis activity, growth and productivity.
507 Several mechanisms have been identified to protect or repair PSII under conditions of
508 excess light energy (Müller *et al.*, 2001; Takahashi *et al.*, 2007, 2009; Huang *et al.*, 2012).
509 Among them, leaf movements have been observed in several plant species in response to
510 direct sunlight (Takahashi and Badger, 2011). In a light-avoiding movement known as
511 paraheliotropism, the grapevine leaves orient at an angle parallel to the sun's rays
512 (Iandolino *et al.*, 2013; Keller, 2015). This movement helps to prevent photodamage of
513 PSII and minimizes photoinhibition (Pastenes *et al.*, 2005; Takahashi *et al.*, 2009).
514 Paraheliotropic movements are also observed when environmental conditions change, *e.g.*
515 when exposed to excess light, high temperatures, or drought stress (During, 1988; Pastenes
516 *et al.*, 2005; Iandolino *et al.*, 2013).
517 These grapevine leaf movements are governed *via* common plant mechanisms based on
518 differentially changing cell turgor within the pulvinus. Substantial information about
519 pulvinus structure and function has been gained by studying the nyctinastic leguminous
520 tree *Samanea saman* (Satter *et al.*, 1981; Gorton, 1987a, 1987b; Yu *et al.*, 2001, 2006). In
521 this species, two groups of specialized motor cells arranged in two opposite zones can be
522 distinguished in the pulvinus: the flexor cell, located in the adaxial side; and the extensor
523 cell, located in the abaxial side (Uehlein and Kaldenhoff, 2008). Similar to the guard cells,
524 solute content and ion composition (which are mainly dependent on potassium) induce
525 osmotic water fluxes in the motor cells, allowing them to change their volume and shape
526 according to turgor changes. Accordingly, uptake of K^+ can lift the leaves through swelling
527 of the abaxial extensor cells, concomitant with shrinking of the adaxial flexor cells (Fig.
528 4a). Upon redistribution of potassium ions, the opposite effect takes place: the extensor
529 cells shrink and the flexor cells swell, lowering the position of the leaves (Fig. 4b) (Gorton,
530 1987a and b; Satter *et al.*, 1974). Moreover, our *in situ* hybridization experiments detected
531 an intense expression of *VvK3.1* in this structure, which was restricted to the abaxial side
532 of the pulvinus, where the extensor cells are usually found (Fig. 4c3).
533 Taking into account the unique functional features of *VvK3.1*, we propose that this channel
534 mediates both inward and outward K^+ currents to allow for the influx or efflux of
535 potassium involved in either the swelling or shrinking of extensor cells. The activity of
536 *VvK3.1*-like channels has already been recorded in *Samanea saman* motor cells, with
537 results that support our hypothesis (Moshelion *et al.*, 2002; Yu *et al.*, 2006). Interestingly,
538 pH values recorded in the *Samanea saman* extensor apoplast have been observed to range

539 from 6.5 to 7.2 (Lee and Satter, 1989), which would be compatible with a significant
540 VvK3.1 activity in extensor cells. Since VvK3.1 is only expressed in extensor cells, two
541 alternative hypotheses may be considered for the mechanism that takes place in flexor
542 cells. The first one is that the elasticity of pectin walls in the parenchyma cells of the flexor
543 tissue is sufficient to facilitate and accommodate leaf movements. The second hypothesis
544 speculates that there are other transport systems involved in K⁺ conductance in grapevine
545 flexor cells (Yu *et al.*, 2001; Moshelion *et al.*, 2002).

546 Here, we have provided evidence that the VvK3.1 channel, in addition to its role in
547 grapevine pulvinus functioning, may play a key role in berry loading during grape berry
548 ripening by controlling phloem K⁺ transport. In grape berries, veraison occurs at a time of
549 profound developmental changes. The shift from the symplasmic to the apoplasmic mode
550 of phloem unloading modifies the translocation pathways. The VvK3.1 and VvK1.2
551 (Cuéllar *et al.*, 2013) channels are both expressed in perivascular cells (Fig. S5), and are
552 likely involved in the reorganization of the K⁺ transport mechanisms that take place during
553 the loading of ripening berries. Moreover, the expression of these two channels is
554 upregulated upon drought stress exposure, suggesting a compensatory measure to control
555 K⁺ transport, thereby preventing the decrease of water availability. Our results strongly
556 indicate that a better understanding of the mechanisms regulating K⁺ transport during berry
557 maturation will likely help to stimulate advances in our knowledge of grapevine drought
558 stress adaptation, berry development, and the determinants of fruit acidity and quality.

559

560

561 Acknowledgements:

562 This work was supported by SweetKaliGrape ANR (ANR-33 14-CE20-0002-02). M.N.-C.
563 received a grant from the Marie Curie program (FP7-IEF, grant no. 272390), and M.A.
564 received a scholarship from the Conabex Commission of Madagascar.

565

566 Author contributions:

567 MN-C, MA and SZ performed electrophysiology experiments. TC and IG performed
568 cloning and q-PCR. TC and JLV performed *in situ* hybridization and histological
569 experiments. MB performed rooted cane cultures. BM, NP, MN-C and RG contributed
570 new reagents/analytic tools. IG conceived the project. analyzed the data and drafted the
571 manuscript.

572

573

574

References:

575

576

Ache P, Becker D, Deeken R, Dreyer I, Weber H, Fromm J, Hedrich R. 2001. VFK1, a *Vicia faba* K(+) channel involved in phloem unloading. *Plant J* **27**(6): 571-580.

577

578

Adir N, Zer H, Shochat S, Ohad I. 2003. Photoinhibition - a historical perspective. *Photosynth Res* **76**(1-3): 343-370.

579

580

Chatelet DS, Rost TL, Matthews MA, Shackel KA. 2008a. The peripheral xylem of grapevine (*Vitis vinifera*) berries. 2. Anatomy and development. *J Exp Bot* **59**(8): 1997-2007.

581

582

583

Chatelet DS, Rost TL, Shackel KA, Matthews MA. 2008b. The peripheral xylem of grapevine (*Vitis vinifera*). 1. Structural integrity in post-veraison berries. *J Exp Bot* **59**(8): 1987-1996.

584

585

586

Chérel I, Michard E, Platet N, Mouline K, Alcon C, Sentenac H, Thibaud JB. 2002. Physical and functional interaction of the Arabidopsis K(+) channel AKT2 and phosphatase AtPP2CA. *Plant Cell* **14**(5): 1133-1146.

587

588

589

Choat B, Gambetta GA, Shackel KA, Matthews MA. 2009. Vascular function in grape berries across development and its relevance to apparent hydraulic isolation. *Plant Physiol* **151**(3): 1677-1687.

590

591

592

Conde C, Silva P, Fontes N, Dias A, Tavares RM, Sousa MJ, Agasse A, Delrot S, Gerós H. 2007. Biochemical changes throughout grape berry development and fruit and wine quality. *Food* **1**: 1-22.

593

594

595

Cuéllar T, Azeem F, Andrianteranagna M, Pascaud F, Verdeil JL, Sentenac H, Zimmermann S, Gaillard I. 2013. Potassium transport in developing fleshy fruits: the grapevine inward K(+) channel VvK1.2 is activated by CIPK-CBL complexes and induced in ripening berry flesh cells. *Plant J* **73**(6): 1006-1018.

596

597

598

Cuéllar T, Pascaud F, Verdeil JL, Torregrosa L, Adam-Blondon AF, Thibaud JB, Sentenac H, Gaillard I. 2010. A grapevine Shaker inward K(+) channel activated by the calcineurin B-like calcium sensor 1-protein kinase CIPK23 network is expressed in grape berries under drought stress conditions. *Plant J* **61**(1): 58-69.

600

601

602

603

Davies C, Shin R, Liu W, Thomas MR, Schachtman DP. 2006. Transporters expressed during grape berry (*Vitis vinifera* L.) development are associated with an increase in berry size and berry potassium accumulation. *J Exp Bot* **57**(12): 3209-3216.

604

605

606

Deeken R, Geiger D, Fromm J, Koroleva O, Ache P, Langenfeld-Heyser R, Sauer N, May ST, Hedrich R. 2002. Loss of the AKT2/3 potassium channel affects sugar loading into the phloem of Arabidopsis. *Planta* **216**(2): 334-344.

607

608

609

Deeken R, Sanders C, Ache P, Hedrich R. 2000. Developmental and light-dependent regulation of a phloem-localised K⁺ channel of Arabidopsis thaliana. *Plant J* **23**(2): 285-290.

610

611

612

Dreyer I, Becker D, Bregante M, Gambale F, Lehnen M, Palme K, Hedrich R. 1998. Single mutations strongly alter the K⁺-selective pore of the K(in) channel KAT1. *FEBS Lett* **430**(3): 370-376.

613

614

615

Dreyer I, Gomez-Porrás JL, Riedelsberger J. 2017. The potassium battery: a mobile energy source for transport processes in plant vascular tissues. *New Phytol.* **216**(4):1049-1053

616

617

618

Dreyer I, Michard E, Lacombe B, Thibaud JB. 2001. A plant Shaker-like K⁺ channel switches between two distinct gating modes resulting in either inward-rectifying or "leak" current. *FEBS Lett* **505**(2): 233-239.

619

620

621

Dreyer I, Uozumi N. 2011. Potassium channels in plant cells. *FEBS J* **278**(22): 4293-4303.

622

- 623 **Duchêne E, Dumas V, Jaegli N, Merdinoglu D. 2014.** Genetic variability of descriptors
624 for grapevine berry acidity in Riesling, Gewürztraminer and their progeny.
625 *Australian Journal of Grape and Wine Research* **20**(1): 91-99.
- 626 **During H. 1988.** CO₂ assimilation and phosphorespiration of grapevine leaves: Responses
627 to light and drought. *Vitis* **27**: 199-208.
- 628 **Ehrhardt T, Zimmermann S, Muller-Rober B. 1997.** Association of plant K⁺(in)
629 channels is mediated by conserved C-termini and does not affect subunit assembly.
630 *FEBS Lett* **409**(2): 166-170.
- 631 **Esteban MA, Villanueva MJ, Lissarrague JR. 2001.** Effect of irrigation on changes in
632 the anthocyanin composition of the skin of cv. Tempranillo (*Vitis vinifera* L.) grape
633 berries during ripening. *Journal of the Science of Food and Agriculture*. **81**(4): 409–
634 420.
- 635
- 636 **Famiani F, Farinelli D, Frioni T, Palliotti A, Battistelli A, Moscatello S, Walker RP.**
637 **2016.** Malate as substrate for catabolism and gluconeogenesis during ripening in
638 the pericarp of different grape cultivars. *Biologia Plantarum* **60**(1): 155-162.
- 639 **Findlay N, O, K. J., Nii N, Coombe BG. 1987.** Solute accumulation by grape pericarp
640 cells. IV. Perfusion of pericarp apoplast via the pedicel and evidence for xylem
641 malfunction in ripening berries. *Journal of Experimental Botany* **38**: 668-679.
- 642 **Gajdanowicz P, Michard E, Sandmann M, Rocha M, Correa LG, Ramirez-Aguilar**
643 **SJ, Gomez-Porrás JL, Gonzalez W, Thibaud JB, van Dongen JT, et al. 2011.**
644 Potassium (K⁺) gradients serve as a mobile energy source in plant vascular tissues.
645 *Proc Natl Acad Sci U S A* **108**(2): 864-869.
- 646 **Gorton HL. 1987a.** Water Relations in Pulvini from *Samanea saman*: I. Intact Pulvini.
647 *Plant Physiol* **83**(4): 945-950.
- 648 **Gorton HL. 1987b.** Water Relations in Pulvini from *Samanea saman*: II. Effects of
649 Excision of Motor Tissues. *Plant Physiol* **83**(4): 951-955.
- 650 **Hafke JB, Furch AC, Reitz MU, van Bel AJ. 2007.** Functional sieve element protoplasts.
651 *Plant Physiol* **145**(3): 703-711.
- 652 **Hanana M, Cagnac O, Yamaguchi T, Hamdi S, Ghorbel A, Blumwald E. 2007.** A
653 grape berry (*Vitis vinifera* L.) cation/proton antiporter is associated with berry
654 ripening. *Plant Cell Physiol* **48**(6): 804-811.
- 655 **Held K, Pascaud F, Eckert C, Gajdanowicz P, Hashimoto K, Corratge-Faillie C,**
656 **Offenborn JN, Lacombe B, Dreyer I, Thibaud JB, et al. 2011.** Calcium-
657 dependent modulation and plasma membrane targeting of the AKT2 potassium
658 channel by the CBL4/CIPK6 calcium sensor/protein kinase complex. *Cell Res*
659 **21**(7): 1116-1130.
- 660 **Huang W, Yang SJ, Zhang SB, Zhang JL, Cao KF. 2012.** Cyclic electron flow plays an
661 important role in photoprotection for the resurrection plant *Paraboea rufescens*
662 under drought stress. *Planta* **235**(4): 819-828.
- 663 **Iandolino AB, Pearcy RW, Williams LE. 2013.** Simulating three-dimensional grapevine
664 canopies and modelling their light interception characteristics. *Australian Journal*
665 *of Grape and Wine Research*: n/a-n/a.
- 666 **Ivashikina N, Deeken R, Fischer S, Ache P, Hedrich R. 2005.** AKT2/3 subunits render
667 guard cell K⁺ channels Ca²⁺ sensitive. *J Gen Physiol* **125**(5): 483-492.
- 668 **Jaillon O, Aury JM, Noel B, Policriti A, Clepet C, Casagrande A, Choise N,**
669 **Aubourg S, Vitulo N, Jubin C, et al. 2007.** The grapevine genome sequence
670 suggests ancestral hexaploidization in major angiosperm phyla. *Nature* **449**(7161):
671 463-467.

- 672 **Jones GV, White MA, Cooper OR, Storchmann K. 2005.** Climate Change and Global
673 Wine Quality. *Climatic Change* **73**(3): 319-343.
- 674 **Kanellis AK, Roubelakis - Angelakis KA 1993.** Grape. In: Seymour GB, Taylor JE,
675 Tucker GA eds. *Biochemistry of Fruit Ripening*. Dordrecht: Springer Netherlands,
676 189-234.
- 677 **Keller M 2015.** Partitioning of assimilates. In: Press A ed. *The Science of grapevines:*
678 *Anatomy and Physiology*. UK: Elsevier Inc., 145-187.
- 679 **Keller M, Smith JP, Bondada BR. 2006.** Ripening grape berries remain hydraulically
680 connected to the shoot. *J Exp Bot* **57**(11): 2577-2587.
- 681 **Kennedy JA., Matthews MA., Waterhouse AL. 2002.** Effect of maturity and vine water
682 status on grape skin and wine flavonoids. *Am. J. Enol. Vitic.* **53**: 268-274.
- 683 **Knipfer T, Fei J, Gambetta GA, McElrone AJ, Shackel KA, Matthews MA. 2015.**
684 Water Transport Properties of the Grape Pedicel during Fruit Development:
685 Insights into Xylem Anatomy and Function Using Microtomography. *Plant Physiol*
686 **168**(4): 1590-1602.
- 687 **Kodur S. 2011.** Effects of juice pH and potassium on juice and wine quality, and
688 regulation of potassium in grapevines through rootstocks (*Vitis*): a short review.
689 *Vitis* **50**(1): 1-6.
- 690 **Kuhn C, Grof CP. 2010.** Sucrose transporters of higher plants. *Curr Opin Plant Biol*
691 **13**(3): 288-298.
- 692 **Lacombe B, Pilot G, Michard E, Gaymard F, Sentenac H, Thibaud JB. 2000.** A
693 shaker-like K(+) channel with weak rectification is expressed in both source and
694 sink phloem tissues of Arabidopsis. *Plant Cell* **12**(6): 837-851.
- 695 **Langer K, Ache P, Geiger D, Stünzing A, Arend M, Wind C, Regan S, Fromm J,**
696 **Hedrich R. 2002.** Poplar potassium transporters capable of controlling K+
697 homeostasis and K+-dependent xylogenesis. *Plant J* **32**(6): 997-1009.
- 698 **Lecourieux F, Kappel C, Lecourieux D, Serrano A, Torres E, Arce-Johnson P, Delrot**
699 **S. 2014.** An update on sugar transport and signalling in grapevine. *J Exp Bot* **65**(3):
700 821-832.
- 701 **Lee Y, Satter RL. 1989.** Effects of white, blue, red light and darkness on pH of the
702 apoplast in the *Samanea pulvinus*. *Planta* **178**(1): 31-40.
- 703 **Lefoulon C, Boeglin M, Moreau B, Véry AA, Szponarski W, Dauzat M, Michard E,**
704 **Gaillard I, Chérel I. 2016.** The Arabidopsis AtPP2CA Protein Phosphatase
705 Inhibits the GORK K+ Efflux Channel and Exerts a Dominant Suppressive Effect
706 on Phosphomimetic-activating Mutations. *J Biol Chem* **291**(12): 6521-6533.
- 707 **Marten I, Hoth S, Deeken R, Ache P, Ketchum KA, Hoshi T, Hedrich R. 1999.** AKT3,
708 a phloem-localized K+ channel, is blocked by protons. *Proc Natl Acad Sci U S A*
709 **96**(13): 7581-7586.
- 710 **Michard E, Dreyer I, Lacombe B, Sentenac H, Thibaud JB. 2005a.** Inward rectification
711 of the AKT2 channel abolished by voltage-dependent phosphorylation. *Plant J*
712 **44**(5): 783-797.
- 713 **Michard E, Lacombe B, Poree F, Mueller-Roeber B, Sentenac H, Thibaud JB, Dreyer**
714 **I. 2005b.** A unique voltage sensor sensitizes the potassium channel AKT2 to
715 phosphoregulation. *J Gen Physiol* **126**(6): 605-617.
- 716 **Moran N. 2007.** Osmoregulation of leaf motor cells. *FEBS Lett* **581**(12): 2337-2347.
- 717 **Moshelion M, Becker D, Czempinski K, Mueller-Roeber B, Attali B, Hedrich R,**
718 **Moran N. 2002.** Diurnal and circadian regulation of putative potassium channels in
719 a leaf moving organ. *Plant Physiol* **128**(2): 634-642.

- 720 **Mpelasoka BS, Schachtman DP, Treeby MT, Thomas MR. 2003.** A review of
721 potassium nutrition in grapevines with special emphasis on berry accumulation.
722 *Australian Journal of Grape and Wine Research* **9**: 154-168.
- 723 **Müller P, Li XP, Niyogi KK. 2001.** Non-photochemical quenching. A response to excess
724 light energy. *Plant Physiol* **125**(4): 1558-1566.
- 725 **Nieves-Cordones M, Chavanieu A, Jeanguenin L, Alcon C, Szponarski W, Estaran S,**
726 **Chérel I, Zimmermann S, Sentenac H, Gaillard I. 2014.** Distinct amino acids in
727 the C-linker domain of the Arabidopsis K⁺ channel KAT2 determine its subcellular
728 localization and activity at the plasma membrane. *Plant Physiol* **164**(3): 1415-1429.
- 729 **Pastenes C, Pimentel P, Lillo J. 2005.** Leaf movements and photoinhibition in relation to
730 water stress in field-grown beans. *J Exp Bot* **56**(411): 425-433.
- 731 **Pastenes C, Porter V, Baginsky C, Horton P, Gonzalez J. 2004.** Paraheliotropism can
732 protect water-stressed bean (*Phaseolus vulgaris* L.) plants against photoinhibition. *J*
733 *Plant Physiol* **161**(12): 1315-1323.
- 734 **Philippar K, Buchsenschutz K, Abshagen M, Fuchs I, Geiger D, Lacombe B, Hedrich**
735 **R. 2003.** The K⁺ channel KZM1 mediates potassium uptake into the phloem and
736 guard cells of the C₄ grass *Zea mays*. *J Biol Chem* **278**(19): 16973-16981.
- 737 **Philippar K, Fuchs I, Luthen H, Hoth S, Bauer CS, Haga K, Thiel G, Ljung K,**
738 **Sandberg G, Bottger M, et al. 1999.** Auxin-induced K⁺ channel expression
739 represents an essential step in coleoptile growth and gravitropism. *Proc Natl Acad*
740 *Sci U S A* **96**(21): 12186-12191.
- 741 **Pratelli R, Lacombe B, Torregrosa L, Gaymard F, Romieu C, Thibaud JB, Sentenac**
742 **H. 2002.** A grapevine gene encoding a guard cell K(+) channel displays
743 developmental regulation in the grapevine berry. *Plant Physiol* **128**(2): 564-577.
- 744 **Rienth M, Torregrosa L, Sarah G, Ardisson M, Brillouet JM, Romieu C. 2016.**
745 Temperature desynchronizes sugar and organic acid metabolism in ripening
746 grapevine fruits and remodels their transcriptome. *BMC Plant Biol* **16**(1): 164.
- 747 **Ronzier E, Corratge-Faillie C, Sanchez F, Prado K, Briere C, Leonhardt N, Thibaud**
748 **JB, Xiong TC. 2014.** CPK13, a noncanonical Ca²⁺-dependent protein kinase,
749 specifically inhibits KAT2 and KAT1 shaker K⁺ channels and reduces stomatal
750 opening. *Plant Physiol* **166**(1): 314-326.
- 751 **Sandmann M, Sklodowski K, Gajdanowicz P, Michard E, Rocha M, Gomez-Porrás**
752 **JL, Gonzalez W, Correa LG, Ramirez-Aguilar SJ, Cuin TA, et al. 2011.** The K
753 (+) battery-regulating Arabidopsis K (+) channel AKT2 is under the control of
754 multiple post-translational steps. *Plant Signal Behav* **6**(4): 558-562.
- 755 **Satter RL, Geballe GT, Applewhite PB, Galston AW. 1974.** Potassium flux and leaf
756 movement in *Samanea saman*. I. Rhythmic movement. *J Gen Physiol* **64**(4): 413-
757 430.
- 758 **Satter RL, Guggino SE, Lonergan TA, Galston AW. 1981.** The effects of blue and far
759 red light on rhythmic leaflet movements in *samanea* and *albizzia*. *Plant Physiol*
760 **67**(5): 965-968.
- 761 **Sharma T, Dreyer I, Riedelsberger J. 2013.** The role of K(+) channels in uptake and
762 redistribution of potassium in the model plant *Arabidopsis thaliana*. *Front Plant Sci*
763 **4**: 224.
- 764 **Skłodowski K, Riedelsberger J, Raddatz N, Riadi G, Caballero J, Chérel I, Schulze**
765 **W, Graf A, Dreyer I. 2017.** The receptor-like pseudokinase MRH1 interacts with
766 the voltage-gated potassium channel AKT2. *Sci Rep* **7**: 44611.
- 767 **Takahashi S, Badger MR. 2011.** Photoprotection in plants: a new light on photosystem II
768 damage. *Trends Plant Sci* **16**(1): 53-60.

- 769 **Takahashi S, Bauwe H, Badger M. 2007.** Impairment of the photorespiratory pathway
770 accelerates photoinhibition of photosystem II by suppression of repair but not
771 acceleration of damage processes in Arabidopsis. *Plant Physiol* **144**(1): 487-494.
- 772 **Takahashi S, Whitney SM, Badger MR. 2009.** Different thermal sensitivity of the repair
773 of photodamaged photosynthetic machinery in cultured Symbiodinium species.
774 *Proc Natl Acad Sci U S A* **106**(9): 3237-3242.
- 775 **Uehlein N, Kaldenhoff R. 2008.** Aquaporins and plant leaf movements. *Ann Bot* **101**(1):
776 1-4.
- 777 **Velasco R, Zharkikh A, Troglio M, Cartwright DA, Cestaro A, Pruss D, Pindo M,
778 Fitzgerald LM, Vezzulli S, Reid J, et al. 2007.** A high quality draft consensus
779 sequence of the genome of a heterozygous grapevine variety. *PLoS One* **2**(12):
780 e1326.
- 781 **Véry AA, Nieves-Cordones M, Daly M, Khan I, Fizames C, Sentenac H. 2014.**
782 Molecular biology of K⁺ transport across the plant cell membrane: what do we
783 learn from comparison between plant species? *J Plant Physiol* **171**(9): 748-769.
- 784 **Wada H, Shackel KA, Matthews MA. 2008.** Fruit ripening in *Vitis vinifera*: apoplastic
785 solute accumulation accounts for pre-veraison turgor loss in berries. *Planta* **227**(6):
786 1351-1361.
- 787 **Yu L, Becker D, Levi H, Moshelion M, Hedrich R, Lotan I, Moran A, Pick U, Naveh
788 L, Libal Y, et al. 2006.** Phosphorylation of SPICK2, an AKT2 channel homologue
789 from *Samanea* motor cells. *J Exp Bot* **57**(14): 3583-3594.
- 790 **Yu L, Moshelion M, Moran N. 2001.** Extracellular protons inhibit the activity of inward-
791 rectifying potassium channels in the motor cells of *Samanea saman* pulvini. *Plant*
792 *Physiol* **127**(3): 1310-1322.
- 793 **Zhang XY, Wang XL, Wang XF, Xia GH, Pan QH, Fan RC, Wu FQ, Yu XC, Zhang
794 DP. 2006.** A shift of Phloem unloading from symplasmic to apoplasmic pathway is
795 involved in developmental onset of ripening in grape berry. *Plant Physiol* **142**(1):
796 220-232.
- 797
- 798

799 **Figure legends**

800

801 **Fig. 1:** The grapevine Shaker K⁺ channel family

802 (a) Phylogenetic relationships in the grapevine and *Arabidopsis thaliana* Shaker K⁺
 803 channel families. The Shaker family displays 5 groups in plants (Pilot *et al.*, 2003), named
 804 I through V. The *A. thaliana* Shaker family harboring voltage-dependent K⁺ channels
 805 comprises 9 members: AKT1 (At2g26650), AKT5 (At4g32500) and SPIK (At2g25600) in
 806 group I; KAT1 (At5g46240) and KAT2 (At4g18290) in group II; AKT2 (At4g22200) in
 807 group III; AtKC1 (At4g32650) in group IV; and GORK (At5g37500) and SKOR
 808 (At3g02850) in group V. The grapevine Shaker family also comprises 9 members: VvK1.2
 809 (NP_001268010.1; Cuéllar *et al.*, 2013), VvKT1.1 (CAZ64538; Cuellar *et al.*, 2010),
 810 VvK2.1 (NP_001268073; Pratelli *et al.*, 2002), VvK3.1 (XP_002268924 – this report),
 811 and 5 other members identified by *in silico* screening of the grapevine genome sequence as
 812 VvK4.1 (XP_003631831.1), VvK5.1 (NP_001268087), VvK5.2 (CBI16957.3), VvK5.3
 813 (XP_002282398), and VvK5.4 (XP_002279184). The members belonging to group III are
 814 highlighted in grey.

815 (b) Representation of a Shaker alpha-subunit structure. A functional shaker channel is built
 816 of four alpha-subunits. Each subunit contains six transmembrane domains (S1-S6) and a
 817 pore domain (P) located between the S5 and S6 domains, which contains the hallmark
 818 TXGYGD/E motif imparting K⁺ selectivity. The C terminus region contains various
 819 domains like the C-linker domain, the putative cyclic nucleotide-binding domain (CNBD),
 820 an ankyrin domain (Ank), and a domain rich in hydrophobic and acidic residues named
 821 K_{HA}.

822

823 **Fig. 2: VvK3.1 transcript levels in grapevine organs**

824 Real-time quantitative PCR was performed on total RNA isolated from leaves or roots
 825 from rooted canes, or from leaves, stems, petioles, tendrils, flowers or berries from open
 826 field grapevines grown under standard irrigation.

827 (a) *VvK3.1* transcript levels of leaves, stems, petioles, tendrils and berries collected at fruit
 828 set.

829 (b) *VvK3.1* transcript levels of berries collected at different developmental stages (days
 830 after flowering). Stages corresponding to fruit set and veraison are indicated by arrows.
 831 The mean values and standard errors of two biological replicates are presented.

832

833

834 **Fig. 3: *In situ* localization of *VvK3.1* transcripts in flowers and berries at fruit set and**
 835 **ripening stages**

836 Longitudinal and equatorial sections were hybridized with *VvK3.1* RNA sense probe (left
 837 column: a1, a2, b1, c1, c2) and antisense probe (right columns). Sections hybridized with
 838 the sense probe (negative control) did not show any significant signal. A positive blue
 839 signal was observed in flowers (a), as well as in berries at fruit set (b) and at post-veraison
 840 (c), when the sections were hybridized with *VvK3.1* antisense probe.

841 (a) *Flowers*: signals were detected in the phloem, ovary and ovule. In the ovary, a blue
 842 color was observed in the epidermis bordering the ovarian locule. In the ovule, a strong
 843 signal was detected in the nucellus.

844 (b) *Berries at fruit set*: blue signals were observed in the endosperm and the phloem.

845 (c) *Berries during ripening*: an intense signal was detected in the vascular bundles, where
 846 the expression of *VvK3.1* is restricted to phloem and perivascular cells.

847 CoS, channel of style; E, endosperm; End, endocarp; EOL, epidermis ovarian locule; Ep,
 848 epicarp; II, inner integument; IM, inner mesocarp; Mes, mesocarp; Nu, nucellus; O, ovule;
 849 OC, ovary cavity; OI, outer integument; OM, outer mesocarp; P, pericarp; Pe, perisperm;
 850 Ph, phloem; PVC, perivascular cells; S, style; SC, seed coat; St, stigmas; StB, stigma basis;
 851 VB, vascular bundles; Xy, xylem.

852

853 **Fig. 4. Expression of *VvK3.1* in pulvinus structures located in the petiole**

854 (a) Anatomical position of the pulvinus and cross sections. A vine branch was
 855 photographed before (a1) and after (a2) the onset of drought stress (brought on by stopping
 856 irrigation). Under drought stress, the petiole position dropped, becoming almost
 857 perpendicular to the stem. The positions of pulvinus structures (white arrows) are clearly
 858 visible, with one located toward the stem side and the other toward the leaf side. Cross
 859 sections of the petiole were observed by stereomicroscope (a3) or light microscope after
 860 histological staining (a4).

861 (b) Histological staining of petiole cross sections. Three-micrometer semi-thin sections
 862 were stained with naphthol blue-black and periodic acid-Schiff. Phloem elements are
 863 distinguishable by their dark purple cell walls stained by periodic acid-Schiff (b3). The
 864 pulvinus is composed of thin-walled parenchyma with intercellular spaces arranged around
 865 the vascular bundle (b2, b3).

866 (c) *In situ* hybridizations with the *VvK3.1* RNA sense probe (left column) and antisense
 867 probe (right column) are shown. A negative control was performed with *the VvK3.1* sense
 868 probe and no signal was observed (c1 and c2). When the cross sections were hybridized
 869 with *VvK3.1* antisense probe, intense signals (blue color) were detected in the phloem sap
 870 (c3, c4 and c6) and in the abaxial side of the pulvinus structure (c3, c5 and c6). No signal
 871 was observed on the adaxial side.

872 Ad.s, adaxial side; Ab.s, abaxial side; Ep, epiderm; ICL, innermost cell layer; OCL, outer
 873 cell layer; Ph, phloem; Pul, pulvinus; VB, vascular bundles; Xy, xylem.

874

875 **Fig. 5. Regulation of *VvK3.1* expression in response to drought stress**

876 *VvK3.1* transcript accumulation was analyzed by real-time quantitative PCR on total RNA.
 877 (a) Berries were collected from field-grown 4-year-old plants under controlled irrigation.
 878 Drought stress was applied by decreasing the level of irrigation for 15 days before berries
 879 were collected. At this point, the leaf water potential was then in the range of -0.7 to -0.6
 880 MPa in drought stressed plants, compared with -0.2 MPa in control plants under standard
 881 irrigation. Absolute transcript levels of the control (white bars) or water-stressed berries
 882 (grey bars) were normalized using EF1-alpha transcript signals. (b) Leaves and (c) roots
 883 were collected from rooted canes. The plants were subjected to drought stress by stopping
 884 irrigation for 10 days. Data are expressed relative to *VvK3.1* transcript accumulation in
 885 plant material collected at $t = 0$. All data presented are the means (\pm SE) of two biological
 886 replicates.

887

888 **Fig. 6. Characterization of the grapevine channel *VvK3.1* in *Xenopus* oocytes**

889 (a) Representative current traces in response to voltage-clamp pulses from +70 mV to
 890 -155 mV for *VvK3.1* in 100 mM K^+ solution at pH 6.5. Note that instantaneous and time-
 891 activating inwardly rectifying currents are typically induced upon hyperpolarization.

892 (b) *VvK3.1* currents are dependent on external potassium concentrations. Current-voltage
 893 curves of normalized *VvK3.1* currents are compared at 100 (K100), 50 (K50) and 10 mM
 894 K^+ (K10) at pH 6.5 ($n=6 \pm$ SD). Steady-state currents at the end of voltage pulses as
 895 presented in (a) are plotted against the corresponding applied membrane potentials.
 896 Currents were normalized for each oocyte, setting the current value at -140 mV in K100 to
 897 -1. (c) Inhibition of *VvK3.1* inward currents by 10 mM Cs^+ . Voltage-dependent current
 898 inhibition of absolute mean currents is shown as a current-voltage curve ($n=12 \pm$ SD).

899

900 **Fig. 7: The grapevine channel VvK3.1 is strongly regulated by pH**

901 (a) VvK3.1 currents are regulated by external pH. Current-voltage curves are shown for
 902 normalized VvK3.1 currents in 100 mM K⁺ at pH 5.5, 6.5 and 7.5 (n=15 ± SD). Currents
 903 were normalized for each oocyte, setting the current value at -140 mV in K100 pH 6.5 to -
 904 1. Note that the currents are reduced by external acidification.

905 (b) Proportion (*i.e.* percentage scale) of the time-dependent (grey) and instantaneous
 906 (black) currents as a function of external pH. (n=15 ± SD). Oocytes were injected with
 907 VvK3.1 cRNA and steady-state currents were recorded at -140 mV before analysis. Note
 908 that the proportion of instantaneous current is stronger at pH 5.5 than at pH 7.5.

909

910 **Fig. 8: Activation of VvK3.1 by co-expression of grapevine CIPK/CBL partners in**

911 *Xenopus* oocytes

912 VvK3.1 currents are slightly stimulated by co-expression with VvCIPK02/05 and
 913 VvCBL04, and more significantly stimulated by co-expression with VvCIPK03 and
 914 VvCBL04.

915 (a) Representative current traces in response to voltage-clamp pulses from +70 mV to
 916 -140 mV for control oocytes injected with either water, VvCIPK03/VvCBL04,
 917 VvCIPK02/05/VvCBL04, VvK3.1, alone, or VvK3.1 with CIPK/CBL partners, in 100 mM
 918 K⁺ solution at pH 6.5.

919 (b) Current-voltage curves of absolute VvK3.1 currents from the same oocyte batch on the
 920 same day are compared for expression of VvK3.1 alone or with the corresponding partners
 921 in 100 mM K⁺ (K100) at pH 6.5 (n=10 mean ± SD). Steady-state currents at the end of the
 922 voltage pulses are plotted against the corresponding applied membrane potentials.

923 (c) Proportion of the time-dependent (grey) and instantaneous (black) currents calculated
 924 from steady-state current as recorded in (b) (n=16-17; mean ± SD). Note that there was no
 925 modification of the relative proportion of the instantaneous and time-dependent
 926 components of the VvK3.1 currents.

927

928 **Supporting Information**

929

930 **Table S1:** Primers used in this study.

931 **Fig. S1:** Localization of *VvK3.1* transcript in leaves by *in situ* hybridization.

932 **Fig. S2:** Localization of *VvK3.1* transcripts in roots by *in situ* hybridization.

933 **Fig. S3:** Reversal potential and Ba²⁺ inhibition.

934 **Fig. S4:** Phylogenetic relationships of CIPKs and CBLs in Arabidopsis and grapevine.

935 **Fig. S5:** Expression of *VvK3.1* and *VvK1.2* in perivascular cells as revealed by *in situ*

936 hybridization

937

938

939

940

941

For Peer Review

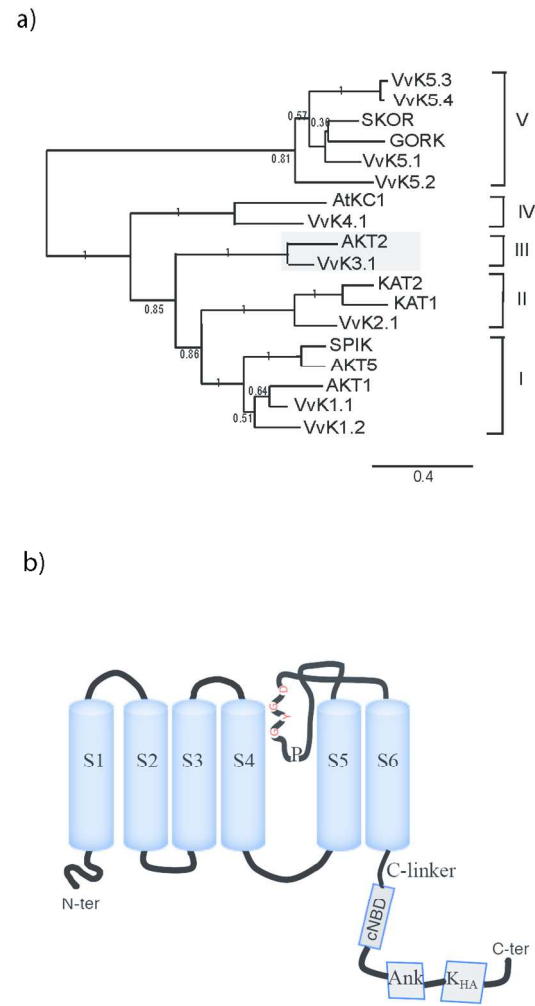


Figure 1

Fig.1: The grapevine Shaker K⁺ channel family

210x297mm (165 x 174 DPI)

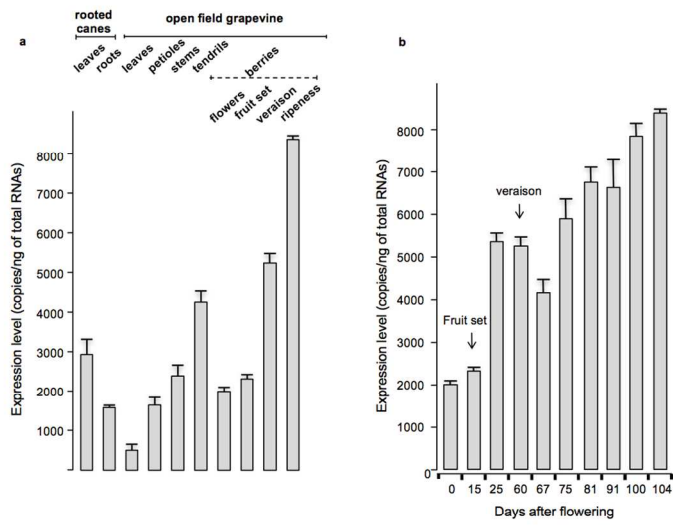


Figure 2

Fig. 2: VvK3.1 transcript levels in grapevine organs

209x297mm (150 x 150 DPI)

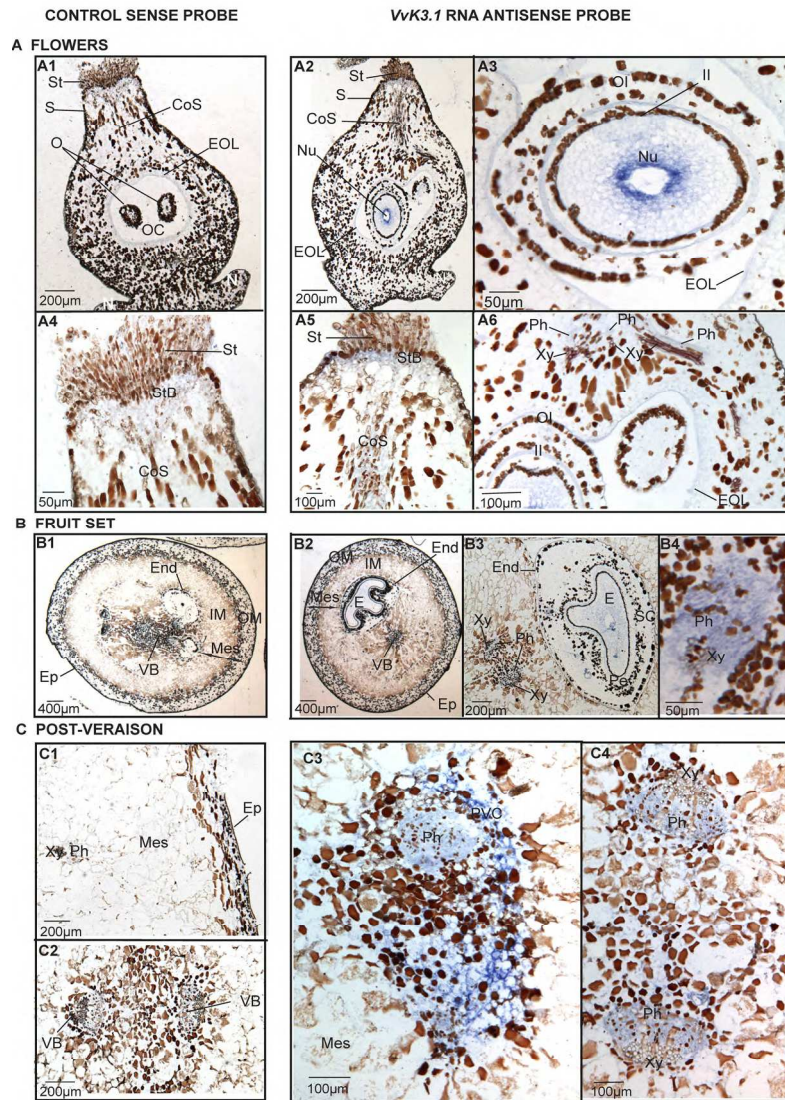


Figure 3

Fig. 3: In situ localization of VvK3.1 transcripts in flowers and berries at fruit set and ripening stages

300x450mm (150 x 150 DPI)

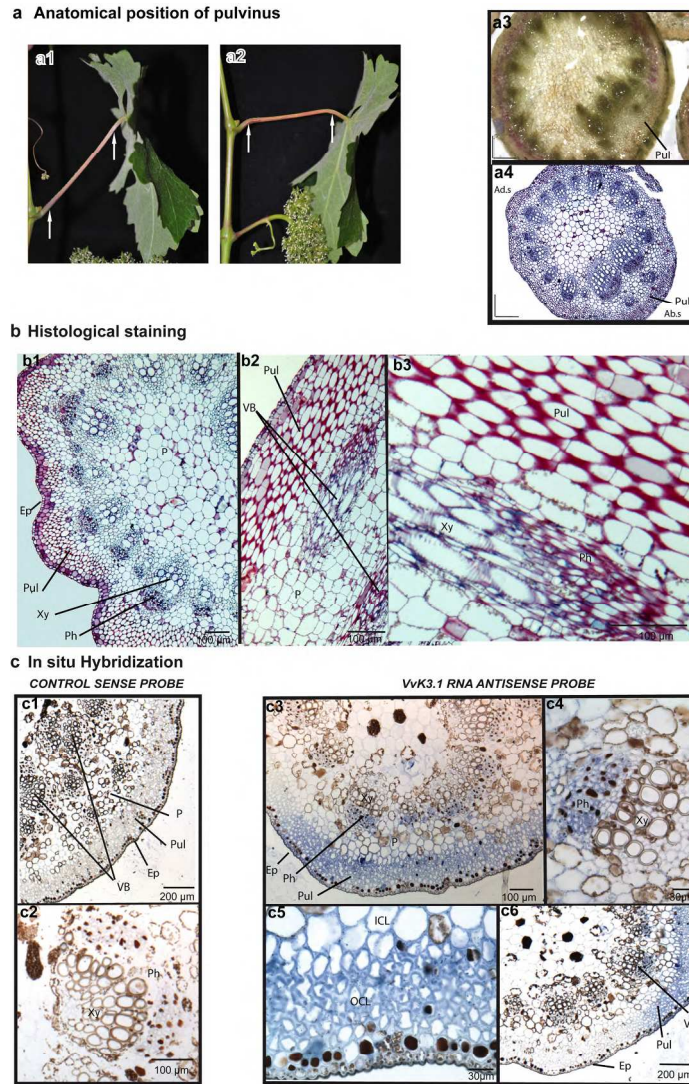


Figure 4

Fig. 4. Expression of VvK3.1 in pulvinus structures located in the petiole

306x522mm (150 x 150 DPI)

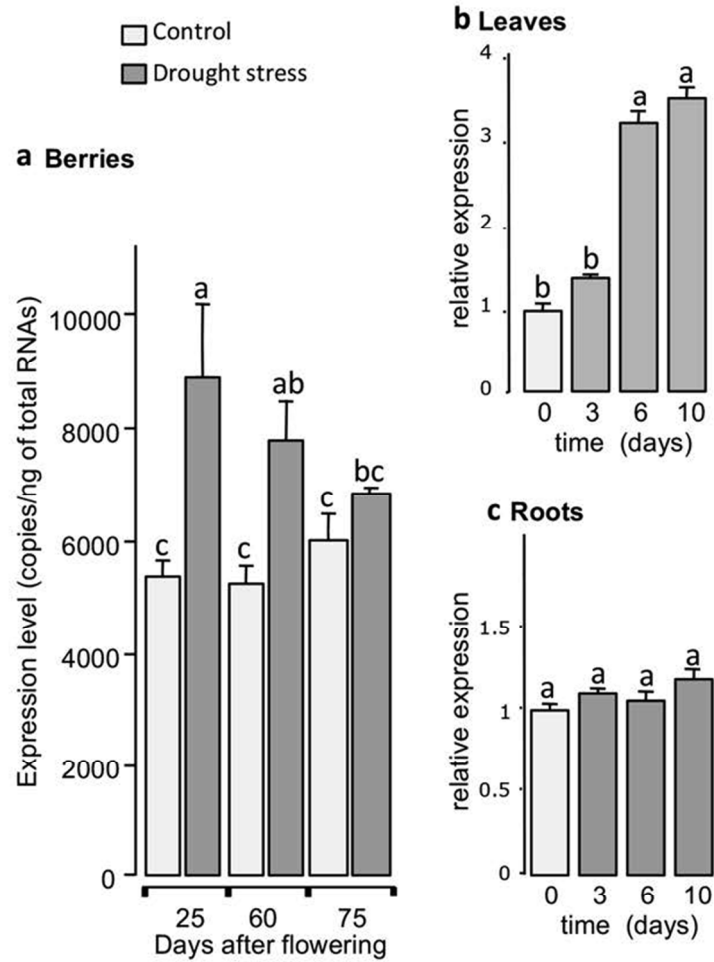


Figure 5

Fig. 5. Regulation of VvK3.1 expression in response to drought stress

160x263mm (100 x 100 DPI)

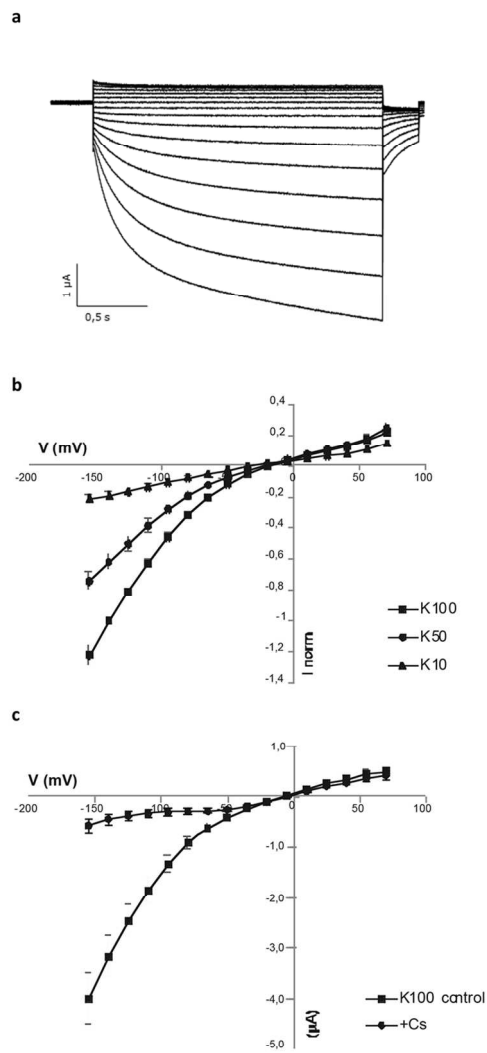


Figure 6

Fig. 6. Characterization of the grapevine channel VvK3.1 in *Xenopus* oocytes

295x546mm (300 x 300 DPI)

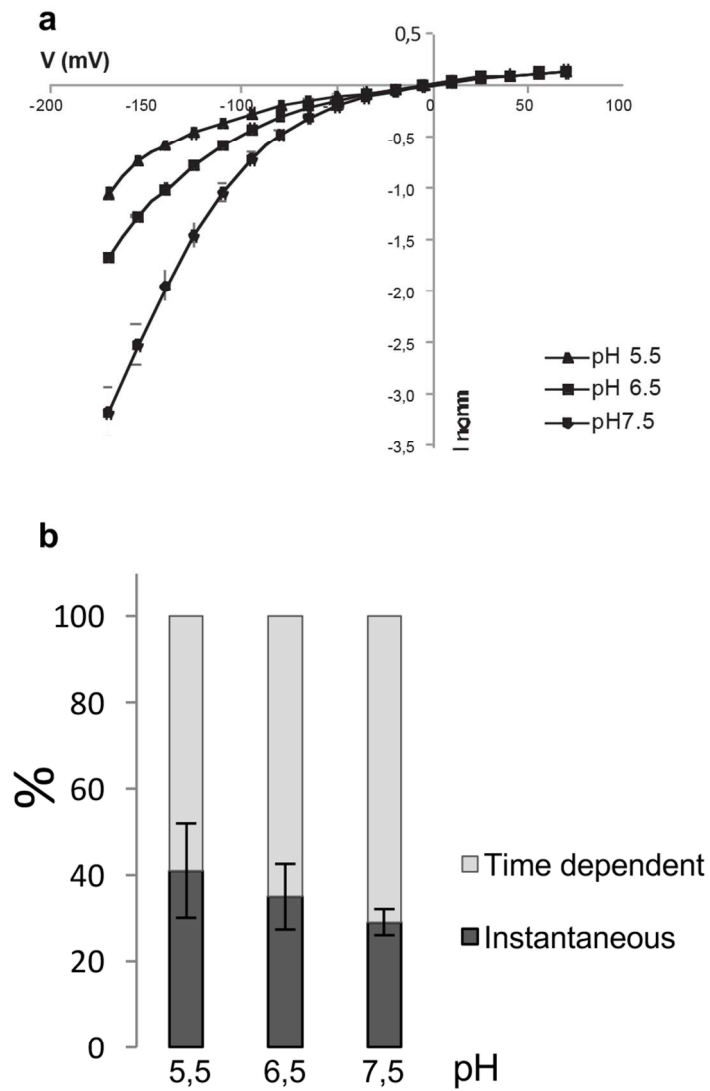


Figure 7

Fig. 7: The grapevine channel VvK3.1 is strongly regulated by pH

263x441mm (300 x 300 DPI)

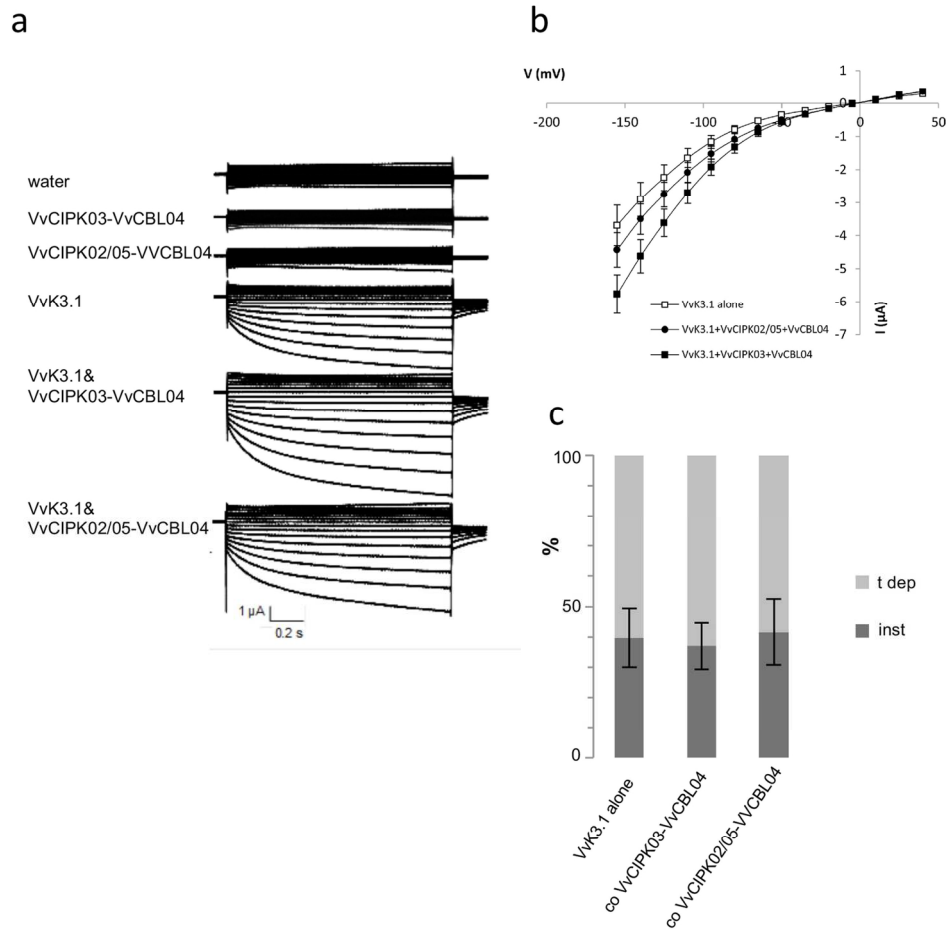


Figure 8

Fig. 8: Activation of VvK3.1 by co-expression of grapevine CIPK/CBL partners in *Xenopus* oocytes

170x182mm (300 x 300 DPI)